PSB33 protein sustains photosystem II in plant chloroplasts under UV-A light

Citation for the original published paper (version of record):

Nilsson, A., Pencik, A., Johansson, O. et al (2020). PSB33 protein sustains photosystem II in plant chloroplasts under UV-A light. Journal of Experimental Botany, 71(22): 7210-7223. http://dx.doi.org/10.1093/jxb/eraa427

(article starts on next page)

RESEARCH PAPER

PSB33 protein sustains photosystem II in plant chloroplasts under UV-A light

Anders K. Nilsson[1,2,] , **Aleš Pěnčík**[3], **Oskar N. Johansson**[1], **Daniel Bånkestad**[4], **Rikard Fristedt**[5,] , **Marjaana Suorsa**[6,] , **Andrea Trotta**[6,] , **Ondřej Novák**[3], **Fikret Mamedov**[7,] , **Eva-Mari Aro**[6,] and **Björn Lundin Burmeister**[1,8,*,]

[1] Department of Biological and Environmental Sciences, University of Gothenburg, Box 461, SE-405 30 Gothenburg, Sweden

[2] Section for Ophthalmology, Department of Clinical Neuroscience, Institute of Neuroscience and Physiology, Sahlgrenska Academy, University of Gothenburg, Gothenburg, Sweden

[3] Laboratory of Growth Regulators, Institute of Experimental Botany of the Czech Academy of Sciences & Faculty of Science of Palacký University, Šlechtitelů 27, CZ-78371 Olomouc, Czech Republic

[4] Heliospectra AB, Fiskhamnsgatan 2, SE-414 58, Gothenburg, Sweden

[5] Chalmers University of Technology, Department of Biology and Biology Engineering, Division of Food and Nutrient Science, SE-41296, Gothenburg, Sweden

[6] Department of Biochemistry, Molecular Plant Biology, FI-20014 University of Turku, Turku, Finland

[7] Molecular Biomimetics, Department of Chemistry – Ångström Laboratory, Uppsala University, 751 20 Uppsala, Sweden

[8] Independent researcher, Gamlestadstorget 28, 41513, Gothenburg, Sweden

* Correspondence: bjorn.lundin.burmeister@gmail.com

Abstract

Plants can quickly and dynamically respond to spectral and intensity variations of the incident light. These responses include activation of developmental processes, morphological changes, and photosynthetic acclimation that ensure optimal energy conversion and minimal photoinhibition. Plant adaptation and acclimation to environmental changes have been extensively studied, but many details surrounding these processes remain elusive. The photosystem II (PSII)-associated protein PSB33 plays a fundamental role in sustaining PSII as well as in the regulation of the light antenna in fluctuating light. We investigated how PSB33 knock-out Arabidopsis plants perform under different light qualities. *psb33* plants displayed a reduction of 88% of total fresh weight compared to wild type plants when cultivated at the boundary of UV-A and blue light. The sensitivity towards UV-A light was associated with a lower abundance of PSII proteins, which reduces *psb33* plants' capacity for photosynthesis. The UV-A phenotype was found to be linked to altered phytohormone status and changed thylakoid ultrastructure. Our results collectively show that PSB33 is involved in a UV-A light-mediated mechanism to maintain a functional PSII pool in the chloroplast.

Key words: Arabidopsis, blue light, photoinhibition, photosystem II, state transition, thylakoid membrane, UV light.

Introduction

The light energy absorbed from the sun is not always beneficial for plants—in excess or under periods of environmental stress, the light causes inhibition of photosystem II (PSII) activity that may result in damage to the photosynthetic apparatus, a phenomenon referred to as photoinhibition (Kok, 1956; Li *et al.*, 2018). To minimize photoinhibition, plants have evolved

protective mechanisms that ensure functional photosynthesis under light stress conditions (Long *et al.*, 1994; Scheller and Haldrup, 2005; Sarvikas *et al.*, 2006; Yamamoto, 2016). These responses include limiting and dissipation of excess of absorbed light energy, and damage control by scavenging reactive oxygen species (ROS).

The thylakoid PSII auxiliary protein PHOTOSYSTEM II PROTEIN 33 (PSB33, AT1G71500) plays a specific role in the regulation of photoinhibition. PSB33 influences PSII–LHCII supercomplex organization in Arabidopsis (Fristedt *et al.*, 2015), and plants devoid of PSB33 display reduced state transition, i.e. ability to distribute excitation energy between the two photosystems (Fristedt *et al.*, 2017). Furthermore, *psb33* mutants show stunted growth in moderate, high, and fluctuating light (Fristedt *et al.*, 2015, 2017).

When we started cultivating *psb33* mutant plants in our new growth facility, we were unable to reproduce our previous finding that the mutant grows more slowly than wild type under standard conditions (Fristedt *et al.*, 2015). Instead of the expected 50% reduction in fresh weight compared with wild type, *psb33* mutants grew to almost similar size (see Supplementary Fig. S1 at *JXB* online). We hypothesized that this variability in the size of *psb33* is attributed to light spectral differences since the light intensity was identical between these two experiments.

Photoinhibition in plants is initiated by photoinactivation of PSII and is followed by a repair cycle of the damaged subunits. There is currently no consensus regarding how photoinactivation of PSII is initiated and sensed by the plant. The two leading hypotheses, which are not mutually exclusive, are (i) the acceptor-side PSII photoinhibition mechanism induced by singlet oxygen in excessive light, and (ii) the donor-side PSII photoinhibition occurring via light absorbed by the Mn_4O_5Ca cluster of PSII and occurring even in very low light intensities (Aro *et al.*, 1993; Zavafer *et al.*, 2015). However, from studies on the action spectrum of PSII photoinactivation, it is evident that the extent of photoinhibition is wavelength dependent and that light in the UV region of the spectrum (100–400 nm) causes the strongest photoinactivation of PSII (Jones and Kok, 1966; Sarvikas *et al.*, 2006; Takahashi *et al.*, 2010), predominantly targeting the Mn_4O_5Ca cluster of the reaction center and the acceptor side of PSII (Hakala *et al.*, 2005; Ohnishi *et al.*, 2005). Thus, non-photochemistry wavelengths can substantially affect PSII photoinhibition.

The relative excitation pressure on the two photosystems, PSI and PSII, changes depending on light intensity and spectral properties, and the inability to appropriately distribute the light energy between the photosystems may lead to photoinhibition (Bellafiore *et al.*, 2005). Plants can reallocate a fraction of the light-harvesting antenna complex II (LHCII) between PSI and PSII through a process known as state transition (Allen *et al.*, 1981; Adamska *et al.*, 1992). The phosphorylation of the LHCII antenna proteins turns on this reallocation. (Mekala *et al.*, 2015). High excitation pressure on PSII activates the serine–threonine kinase STN7 that phosphorylates LHCII proteins (Bellafiore *et al.*, 2005; Fristedt and Vener, 2011; Trotta *et al.*, 2016). This results in enhanced delivery of excitation energy from LHCII to PSI, thus increasing its light-harvesting

capacity (state II). Over-excitation of PSI, on the other hand, triggers the dephosphorylation of LHCII by the PPH1/TAP38 phosphatase (Pribil *et al.*, 2010; Shapiguzov *et al.*, 2010). Dephosphorylated LHCII associates with PSII to increase its capacity to absorb energy (state I). Under artificial illumination, state I is induced by low-intensity light (Rintamäki *et al.*, 2000) as well as red (636–700 nm) and blue (400–500 nm) light (Bellafiore *et al.*, 2005; Trotta *et al.*, 2016). Far-red light (700–780 nm) preferentially excites PSI and triggers state II (Adamska *et al.*, 1992; Bonardi *et al.*, 2005).

Repair of photodamaged PSII proteins is efficient and under strict quality control, especially of the D1 subunit. This photoinhibition–repair cycle follows a sequential series of highly regulated steps: monomerization of damaged PSII dimers, migration of PSII monomers from appressed to unappressed thylakoid regions, degradation of the damaged D1 protein by FtsH protease, and finally, *de novo* production of D1 subunit insertion into PSII monomers (Ohad *et al.*, 1984; Yoshioka–Nishimura and Yamamoto, 2014). Phosphorylation of the PSII core proteins by the STN8 kinase is important for the repair cycle, influencing the disassembly of the damaged PSII dimer and protecting D1 protein from excess degradation (Tikkanen *et al.*, 2008; Fristedt *et al.*, 2009; Kato and Sakamoto, 2014).

Apart from directly fueling photochemistry, light of different colors and intensities serves as cues during plant development and growth. A large number of photoreceptors allow plants to sense light over a broad spectrum of wavelengths, from UV-B (280–320 nm) to far-red. Phytochromes absorb red and far-red light in the 600–750 nm region and play central roles in plant germination, de-etiolation, stomata development, flowering, shade avoidance, and senescence (Wang and Wang, 2015). Blue and UV light are perceived and effectively transduced as a signal by the photoreceptor families cryptochromes (400–500 nm), phototropins (320–500 nm), zeitlupes (450–520 nm) and UV-B photoreceptors (280–320 nm) (Christie *et al.*, 2015). These photoreceptors control processes that include photomorphogenesis, flowering, circadian period, phototropism, and stomata opening. Signaling pathways downstream of the photoreceptors often integrate with hormone networks and influence their levels (Chaiwanon *et al.*, 2016). Although well studied, there is limited evidence linking photoreceptors directly to regulation of photosynthesis. Photoprotective mechanisms identified in green algae and cyanobacteria have been tied to UV and/or blue light perception by photoreceptors (Kirilovsky and Kerfeld, 2013; Allorent *et al.*, 2016; Petroutsos *et al.*, 2016). Further, blue light perception in diatoms increases their photoprotective potential (Schellenberger Costa *et al.*, 2013). However, these are aquatic organisms exposed to an environment where blue light dominates. In land plants, phototropins activated by blue light stimulate the relocation of chloroplast (Goh, 2009). This process acts to distribute PSII damage among the different cell layers of the leaf in high light (Cazzaniga *et al.*, 2013). More indirectly, blue and UV-A (320–400 nm) light play a role in the regulation of the PSII complex as they stimulate the expression of genes encoding light-harvesting chlorophyll *a/b*-binding proteins (Lhcbs) (Folta and Kaufman, 1999) and a special class of PSII core proteins (D2 and CP43; *PSBD–PSBC*) (Christopher and Mullet, 1994).

Here, we aimed to investigate if changes in light quality affect growth and photosynthetic responses in *psb33* mutant plants. We found that the *psb33* plants show a conditional dwarf phenotype when cultivated under blue light, specifically in UV-A or near UV-A light. This UV-A light-dependent phenotype was found to be associated with low levels of PSII proteins, abnormal thylakoid ultrastructure, and changed phytohormone levels. We suggest that PSB33 is involved in a UV light-mediated mechanism to maintain an efficient PSII repair by regulating the *de novo* synthesis of PSII.

Material and methods

Plant material and growth conditions

Arabidopsis seeds were sown on soil and vernalized at 4 °C for 2 d before transfer to climate-controlled growth chambers (CLF PlantMaster, Plant Climatics, Wertingen, Germany). The plants were grown under a 12 h photoperiod at 20 °C/18 °C light/dark in 60% relative humidity. Seedlings were transplanted into individual pots after 10 d and moved to chambers with LED lamps after an additional 4 d. All mutants and wild type used in the study were in the Columbia-0 genetic background, previously described for *psb33-3* (Fristedt *et al.*, 2015), *stn7* (Bellafiore *et al.*, 2005), *stn8* and *stn7stn8* (Bonardi *et al.*, 2005), *tap38* (Pribil *et al.*, 2010), *amiLhcb1* and *amiLhcb2* (Pietrzykowska *et al.*, 2014), *psbw* (García-Cerdán *et al.*, 2011), *psaI* (Lunde *et al.*, 2000), *pgr5* (Munekage *et al.*, 2002), and *npq4* (Johnson and Ruban, 2010). The LED lights were provided by Heliospectra L4A lamps (Heliospectra, Gothenburg, Sweden) with diode peak wavelengths at 400, 420, 450, 530, 630, 660, and 735 nm. For the experiment with the 385 nm LEDs, Heliospectra RX30 lamps were used. Full light spectra were recorded with a JAZ spectrometer (Ocean Optics, Dunedin, FL, USA). Lamps were set up to ensure an even light distribution of the different colors. For example, when blue and red light were combined, 50% of the total photon flux was provided by blue LEDs and 50% by red LEDs.

Pigment content, hormone analysis, and chlorophyll a fluorescence

Chlorophyll and carotenoids were extracted from leaf discs in 95% (v/v) ethanol for 10 min at 60 °C, and concentrations were determined spectrophotometrically (Lichtenthaler and Wellburn, 1983). Plant hormone levels were determined from leaf discs (12 mm diameter) as described (Floková *et al.*, 2014).

Chlorophyll *a* fluorescence parameters were recorded with a Pocket PEA Chlorophyll Fluorimeter (Hansatech Instruments Ltd, King's Lynn, UK). The maximum quantum efficiency of Photosystem II (F_v/F_m, calculated as $(F_m–F_0)/F_m$) and performance index (PI_{ABS}) (Strasser *et al.*, 2004) were determined in attached leaves dark-acclimated for 20 min in room temperature with 1 s measuring light with the intensity of 3500 µmol m^{-2} s^{-1}.

Thylakoid membrane preparation, SDS-PAGE, and immunoblotting

For extraction of whole leaf proteins, tissue (approximately 200 mg) was frozen in liquid nitrogen, grounded into a fine powder, mixed with buffer (100 mM Tris–HCl pH 8.0, 25 mM EDTA pH 8.0, 250 mM NaCl, 0.75% SDS (v/v), 1 mM DTT, 10 mM NaF; 1× Protease Inhibitor Cocktail Set I (Calbiochem, Merck KGaA, Darmstadt, Germany)) and denatured at 68 °C for 10 min. Centrifugation removed cellular debris, and chlorophyll content was determined as described (Porra *et al.*, 1989). Proteins were loaded on 5%/14% stacking/separating acrylamide gels based on chlorophyll content (100–500 ng µl^{-1} depending on the expected abundance of the protein). SDS-PAGE separation, protein transfer to polyvinylidene difluoride membranes, and detection were as described

(Fristedt *et al.*, 2015). Antibodies used in this work were all from Agrisera Antibodies (Vännäs, Sweden): PsaB, PsaA, RbscL, PsbA, PsbD, Lhcb2-P (AS13 2705), Lhcb2 (AS01 003), Lhcb1-P (AS13 2704), and Lhcb1 (AS01 004).

Staining for reactive oxygen species

Staining for H_2O_2 was performed as previously described with minor modifications (Daudi and O'Brien, 2012). Briefly, seedlings were vacuum inoculated in 10 mM Na_2HPO_4–3,3′-diaminobenzidine (Daudi and O'Brien, 2012) staining solution at approximately 100 mbar for 2 min. After 2 h in darkness, the seedlings were destained in 96% (v/v) ethanol overnight and photographed. Staining for superoxide radicals was performed similarly but using 0.1% nitroblue tetrazolium in 50 mm Na_2HPO_4 (pH ~7).

Transmission electron microscopy

Leaves from plants grown in fluorescent white, red, or blue light were collected 2 h after the onset of light following a 14 h night period. Tissue preparation and imaging were as described (Herdean *et al.*, 2016).

PSII electron transfer properties

Electron transfer properties in PSII were measured by flash-induced variable fluorescence, thermoluminescence, and low-temperature electron paramagnetic resonance (EPR) spectroscopy in thylakoid membranes isolated from wild type and *psb33* mutant plants. Fluorescence decay kinetics were measured using an FL3000 dual modulation kinetic fluorometer, and the thermoluminescence signal was measured using a TL200/PMT thermoluminescence system (both from Photon System Instruments, Brno, Czech Republic) as described in Volgusheva *et al.* (2016).

Low-temperature EPR was measured in an X-band ELEXSYS 500 spectrometer using a SuperX EPR049 microwave bridge and a Bruker 4122SHQE super high-Q cavity (Bruker BioSpin). The system was fitted with a 900-cryostat and an ITC-503 temperature controller from Oxford Instruments Ltd. The S_2 state multiline signal was induced by illumination at 200 K for 6 min, and full oxidation of cytochrome b_{559} was induced by illumination at 77 K as described in Chen *et al.* (2011). Processing and analysis of EPR spectra were performed with the Bruker Xepr program.

Statistical analyses

Data were processed with Microsoft Excel 2010 with the add-in Daniel's XL Toolbox (https://www.xltoolbox.net/) or with IBM SPSS Statistics version 25 (IBM Corp., Armonk, NY, USA). The normality of data was tested using the Shapiro–Wilk method. Non-normally distributed data were log-transformed before parametric tests were performed. Results were considered significant if two-tailed $P<0.05$.

Results

psb33 *mutant plants show a conditional light quality phenotype*

We set out to investigate if the lack of a slow-growth phenotype of *psb33* in our new plant growth facility might be attributed to specific qualitative properties of the fluorescent lights in these chambers (see Supplementary Fig. S1). Therefore, plants were grown under fluorescent white light at a total photon flux density of 120 µmol photons m^{-2} s^{-1} (PFD) for 2 weeks and then transferred to blue (400, 420, 440 nm), red (630, 660 nm), or a combination of blue and red LED lights for an additional 3 weeks (Fig. 1). Wild type and control plants were maintained in the fluorescent white light throughout the

growth period. The total light intensity was kept constant at 120 μmol m^{-2} s^{-1} in all the different spectral conditions (Fig. 1, left panel). To test if the growth phenotype of *psb33* was associated with its inability to induce state transition, the double mutant *stn7stn8* was included as a negative control in the experiment (Tikkanen *et al.*, 2010). After 2 weeks of growth under fluorescent white light, before transfer to LED lights, there was no apparent difference in size between the wild type, *psb33*, and *stn7snt8* (Supplementary Fig. S2).

The *stn7stn8* plants displayed an approximately 20% reduction in fresh weight compared with wild type after 5 weeks in all light conditions except in red light where they grew to a similar size (Fig. 1). *psb33* plants, on the other hand, showed similar fresh weight to wild type in fluorescent white and red light, while a dramatic and statistically significant (one-way ANOVA, *P*<0.001) decrease was observed in blue light. The *psb33* plants grown under a combination of red and blue light displayed an intermediate reduction in fresh weight compared with those cultivated in white or blue light. The growth phenotype of *psb33* in the blue light did not correlate with changes in chlorophyll or carotenoid content (Table 1).

These indicate that the slow–growth phenotype of the *psb33* mutant is related to sensitivity towards blue light. Further, the phenotype appeared not to be a consequence of impaired state transition, since plants lacking the kinases STN7 and STN8 (*stn7stn8* plants) did not respond similarly to *psb33* to the tested light regimes.

Chlorophyll fluorescence characteristics of psb33 in blue and red light

Next, we determined the photosynthetic performance of plants grown under white, blue, and red or a combination of blue and red light (Fig. 2A). The maximum quantum efficiency of photosystem II (F_v/F_m) was similar between the control plants (wild type and the *stn7stn8*) and showed only small variations in the different light conditions. Following our previous results (Fristedt *et al.*, 2015), F_v/F_m in *psb33* was slightly, yet statistically significantly (one-way ANOVA, *P*<0.001) lower than in wild type in white light. However, in blue, red, and combined blue/red light, the F_v/F_m values were reduced by approximately 20% in *psb33*, indicating decreased PSII efficiency
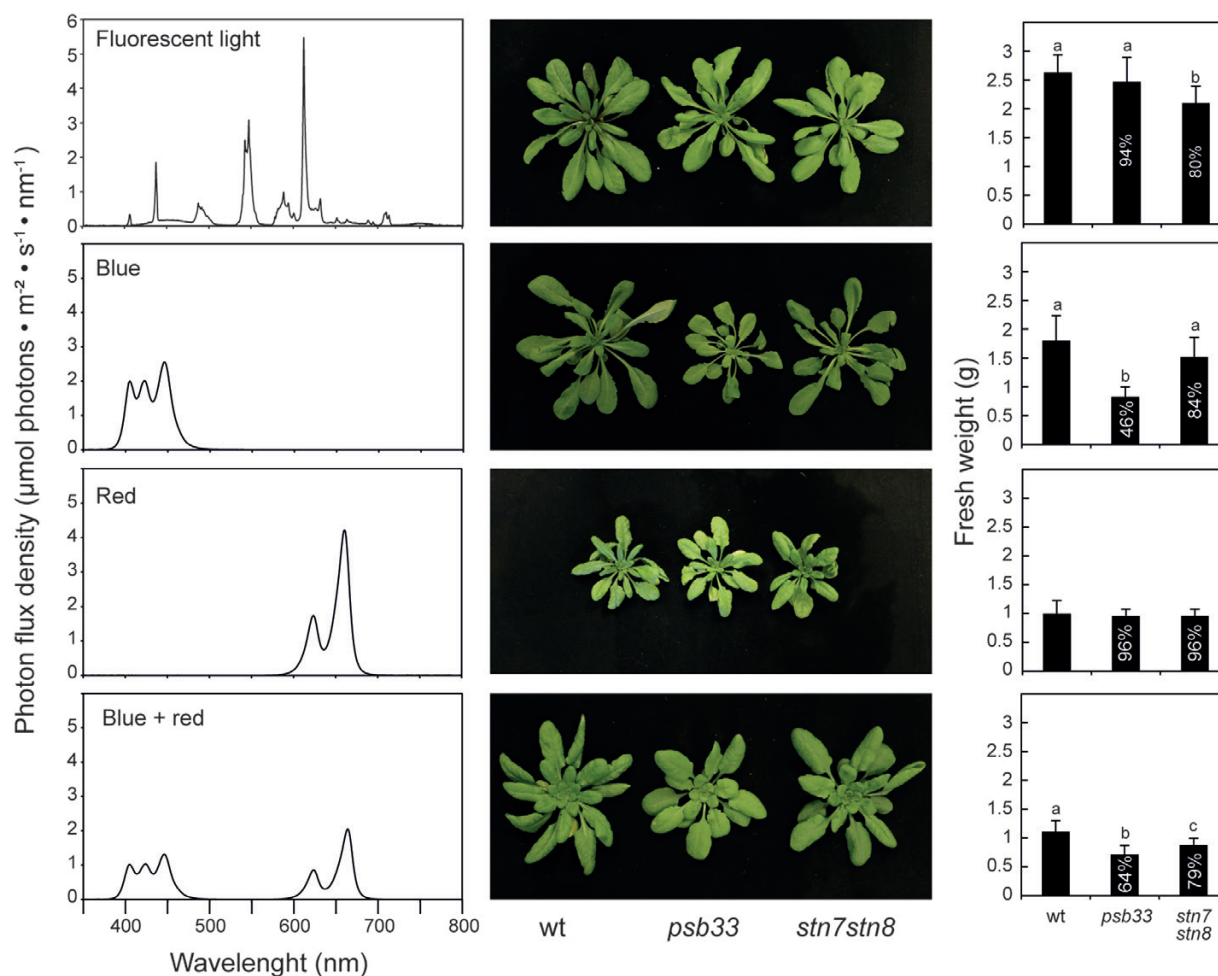

Fig. 1. The growth of the *psb33* is strongly inhibited by blue monochromatic light. Plants were grown for 5 weeks in white fluorescent light at 120 μmols m^{-2} s^{-1}, or alternatively, grown for 2 weeks in white fluorescent light and then transferred to blue or red monochromatic light, or a combination of the two (left panel), and grown for an additional 3 weeks before photographs were taken (middle panel) and fresh weight (FW) determined (right panel). Percentage values in right panel indicate size relative to wild type (WT). Means and standard deviation are shown (*n*=11–24). Letters indicate a statistically significant difference between groups (one-way ANOVA, Bonferroni–Holm *post hoc* test, *P*<0.05). (This figure is available in color at *JXB* online.)

in these conditions (Fig. 2A). In repeated experiments, F_v/F_m was consistently lower in *psb33* plants grown in blue light compared with plants grown in red light. However, this difference was not statistically significant in all experiments (data not shown). The performance index parameter (PI_{ABS}) is an overall parameter of plant vitality and a sensitive index to evaluate stress (Kalaji *et al.*, 2014). PI_{ABS} takes into account the concentration of active reaction centers and the force of the light and dark reactions (Strasser *et al.*, 2000). Although there was some variability between replicates, *stn7stn8* plants largely displayed similar PI_{ABS} to the wild type in all light conditions (see Supplementary Fig. S3). However, *psb33* plants grown in blue, red, and the combination of blue and red light displayed

a decrease in PI_{ABS} in comparison to *psb33* plants grown in fluorescent white light.

To further explore the response of *psb33* to blue and red light. Plants grown in fluorescent white light were transferred to blue and red light, and F_v/F_m was determined at intervals for up to 3 d (Fig. 2B, C). Recovery of the plants was assessed by monitoring the chlorophyll fluorescence after the transfer of plants back to white light. Both blue and red light induced a fast decrease of the F_v/F_m ratio, which reached similar values as in the long-term acclimated plants after 3 d. Following 3 d of recovery in white light, F_v/F_m completely reverted to steady-state values again, showing that these effects were reversible (Fig. 2B, C).

Table 1. Pigment composition in plants grown in different lights.

Light	Total Chl (mg g^{-1})		Carotenoids (mg g^{-1})		Chl *a/b*	
	WT	*psb33*	WT	*psb33*	WT	*psb33*
Fluorescent white	1.11±0.03	0.92±0.07**	0.23±0.01	0.18±0.02**	3.97±0.07	3.85±0.03**
Blue	0.87±0.07	0.74±0.08*	0.18±0.01	0.16±0.02	4.71±0.07	4.33±0.42
Red	0.96±0.23	0.96±0.09	0.20±0.05	0.21±0.02	4.61±0.09	4.63±0.20
Blue and red	1.07±0.09	1.07±0.09	0.22±0.02	0.23±0.02	4.57±0.05	4.46±0.13

Pigment composition was determined in leaf tissue from 5-week-old plants. Plants were grown for 2 weeks in white fluorescent light and then transferred to LED chambers emitting light of different wavelengths of either blue (400, 420, 440 nm) or red (630, 650 nm) light, or a combination of the two and grown for an additional 3 weeks. Control plants were kept in white fluorescent light throughout the growth period. Asterisks indicate statistically significantly difference from wild type under the specified growth condition (*P<0.05, **P<0.01, Student's t-test, n=6). Chl, chlorophyll.
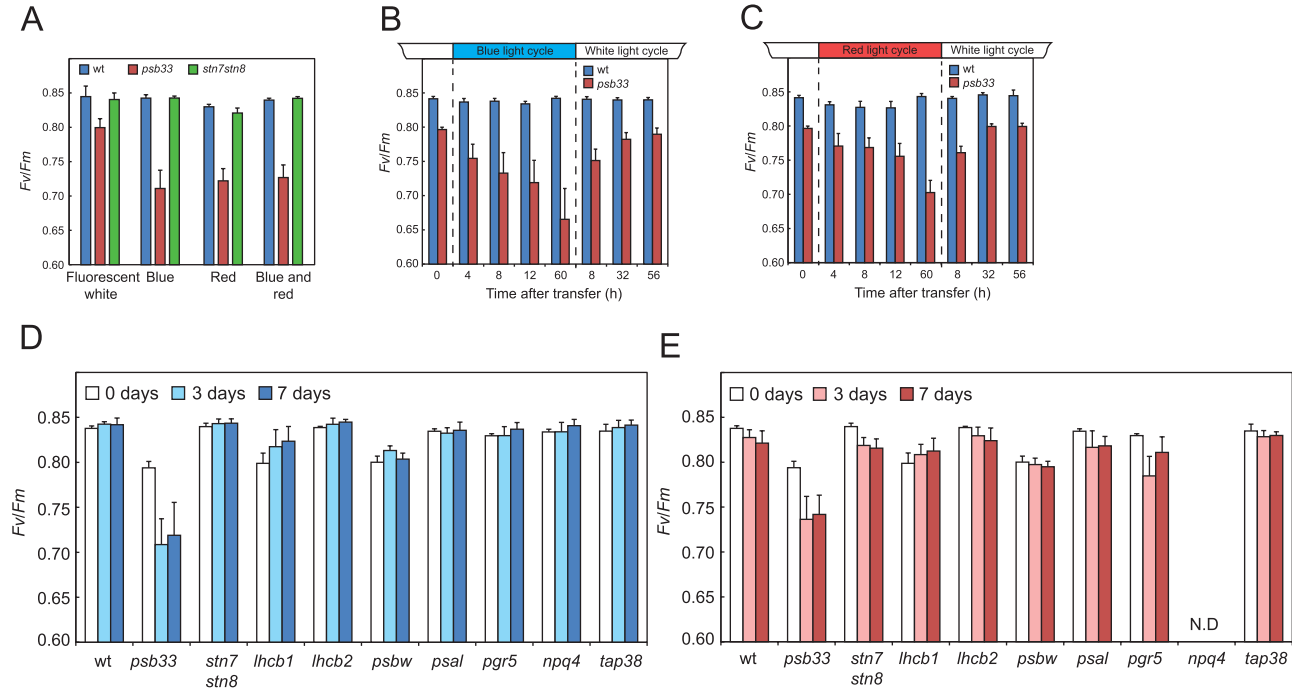

Fig. 2. F_v/F_m in plants under blue and red monochromatic light. (A) Plants were grown for 5 weeks in fluorescent white light at 120 µmols m^{-2} s^{-1}, or alternatively, grown for 2 weeks in fluorescent white light and then transferred to LED growth chambers emitting light in different wavelengths of either blue (400, 420, 440 nm) or red (630, 650 nm) light, or a combination of the two, and grown for an additional 3 weeks before F_v/F_m was determined (n=14–20). (B, C) Plants were grown for 4 weeks in fluorescent white light and then transferred to LED growth chambers emitting light at different wavelengths of either blue (400, 420, 440 nm) (B) or red (630, 660 nm) light (C) and kept for 3 d, then returned to fluorescent white light for 3 d. F_v/F_m values were determined at regular intervals (n=12). (D, E) Plants were grown for 4 weeks in fluorescent white light and then transferred LED growth chambers emitting light in different wavelengths of either blue (400, 420, 440 nm) (D) or red (630, 660 nm) light (E) and F_v/F_m was measured before (0), 3 and 7 d after transfer (n=12–15). ND, not determined. Means and standard deviation are shown. (This figure is available in color at *JXB* online.)

Chlorophyll fluorescence phenotype of psb33 *is not found in other related photosynthetic mutants*

To gain insight into the mechanism behind the strong response of the *psb33* plants to blue and red light, we compared the performance of *psb33* under these light treatments to that of well-characterized photosynthesis mutants. Specifically, mutants lacking components of the photosynthetic machinery associated with excitation energy transfer were selected and compared with *psb33* (Fig. 2D, E). The kinases STN7 and STN8, and phosphatase TAP38 regulate the phosphorylation status of PSII core and LHCII proteins (Bellafiore *et al.*, 2005; Bonardi *et al.*, 2005; Pribil *et al.*, 2010; Shapiguzov *et al.*, 2010). The *stn7*, *stn8*, te *stn7stn8*, and *tap38* mutants have reduced state transition capacity and differ in sensitivity to high or fluctuating light (Fristedt *et al.*, 2009; Tikkanen *et al.*, 2010). The *lhcb1* and the *lhcb2* mutants, corresponding to plants deficient in Lhcb1 and Lhcb2, respectively, show altered antenna and thylakoid structure, impaired state transition, and reduced NPQ (Pietrzykowska *et al.*, 2014). The *npq4* mutant is devoid of the protein PsbS and lacks the qE component of NPQ; it is sensitive to photoinhibition (Li *et al.*, 2002) and fluctuating light (Külheim *et al.*, 2002). PsbS has also been proposed to play a role in energy distribution between the two photosystems (Jajoo *et al.*, 2014). PsbW plays an important role in PSII function, and the corresponding *psbw* mutant shows destabilized PSII supercomplex organization, decreased phosphorylation of PSII core proteins, and faster changes of the redox state of the plastoquinone pool (García–Cerdán *et al.*, 2011). The *psal* mutant lacks a PSI component, shows reduced PSI electron transport rate, and has normal phosphorylation of LHCII but an inability to increase the PSI antenna size in state II light (Lunde *et al.*, 2000). Finally, PGR5 encodes a protein previously thought to be involved in cyclic electron transport around PSI (Munekage *et al.*, 2002), but more recently shown to be involved in regulating proton flux across the thylakoid membrane (Suorsa *et al.*, 2012; Kanazawa *et al.*, 2017). The *pgr5* mutant is unable to induce NPQ, is sensitive to high light, which results in PSI damage (Munekage *et al.*, 2002), shows stunted growth in normal conditions, and is unable to cope with fluctuating light resulting in wilting (Tikkanen *et al.*, 2010).

Comparing the F_v/F_m parameter of all these mutant lines and wild types in response to blue and red light, it is clear that the *psb33* mutant was the only line showing a substantial reduction in photosynthetic performance (Fig. 2D, E). There was no statistical difference in F_v/F_m among the *psb33* plants kept for 3 or 7 d in blue or red light. These results indicated that the observed phenotype of *psb33* is not connected to thylakoid ΔpH-dependent regulation mechanisms since *pgr5* and *npq4* were unaffected under the tested light regimes. The results further strengthened the notion that the phenotype of *psb33* cannot be explained by the lack of photosystem energy distribution-dependent mechanisms since none of the included mutants with impaired ability to phosphorylate PSII core or with altered antenna proteins displayed stress symptoms under red or blue light.

psb33 *plants display altered phytohormone levels in blue and red light*

Plant growth restrictions are commonly associated with defective hormone control. Therefore, we tested if the response of *psb33* plants to blue and red light was accompanied by changes in leaf phytohormone levels (Fig. 3). Our analysis specifically targeted hormones involved in growth and stress signaling: jasmonates (including JA, isoleucine-conjugated JA (JA–Ile), and 12-oxo-phytodienoic acid (*cis*-OPDA)), salicylic acid (SA), indole acetic acid (IAA), and IAA derivatives. SA levels were 3.6 and 5.5 times lower (*P*<0.01, one-way ANOVA, Bonferroni–Holm *post hoc* test) in the mutant compared with wild type in blue and red light, respectively. However, levels were relatively low in both the wild type and *psb33* in all conditions (Fig. 3F). The only statistically significant hormonal change exclusively apparent in *psb33* grown in blue light was a strong accumulation of aspartic acid-conjugated IAA (IAA-Asp) (Fig. 3C).

Blue light induces changes to psb33 *thylakoid ultrastructure*

To further explore the *psb33* growth phenotype and to resolve whether it relates to morphological changes at the microscopic level, the thylakoid ultrastructure of *psb33* plants grown in white, blue, and red light was examined by transmission electron microscopy (Fig. 4). No difference in thylakoid structure was observed between wild type and *psb33* plants grown in fluorescent white or red light. Thylakoids of *psb33* grown in blue light were found to be swollen, showing large luminal spaces at non-appressed regions of the thylakoid membrane (Fig. 4B). Such swollen thylakoids could be observed in a few chloroplasts also from wild type plants taken from blue light. However, virtually all thylakoids from *psb33* plants from blue light displayed such abnormal structures.

UV-A light causes the psb33 *growth phenotype*

Next, we set out to more specifically delineate the light wavelengths causing the deleterious growth phenotype of *psb33* in blue light. Three blue light conditions provided by three different LEDs were tested at the PFD of 120 µmol m^{-2} s^{-1}: 400, 420/440, and 400/420/440 nm (Fig. 5). *psb33* plants cultivated under only 400 nm light only reached 12% of wild type fresh weight at the end of the growth period (Fig. 5A, B), while *psb33* plants in 420/440 nm and 400/420/450 nm light reached 66% and 40%, respectively, of the weight of wild type.

Due to the fact that the 400 nm LED lamp emits light ranging from 391 to 421 nm, with a peak at 404–405 nm, we suspected that light in the UV-A region was the main cause of the dwarf phenotype of *psb33* grown in blue light (Figs 1, 5; Supplementary Fig. S4). Growing plants in 385 nm UV-A light corroborated this finding: *psb33* plants displayed strong growth restriction compared with the wild type in this light condition (Supplementary Fig. S5). Chlorophyll *a* fluorescence measurements showed a drastic reduction in quantum efficiency (F_v/F_m) of PSII and PI$_{ABS}$ in *psb33* plants grown
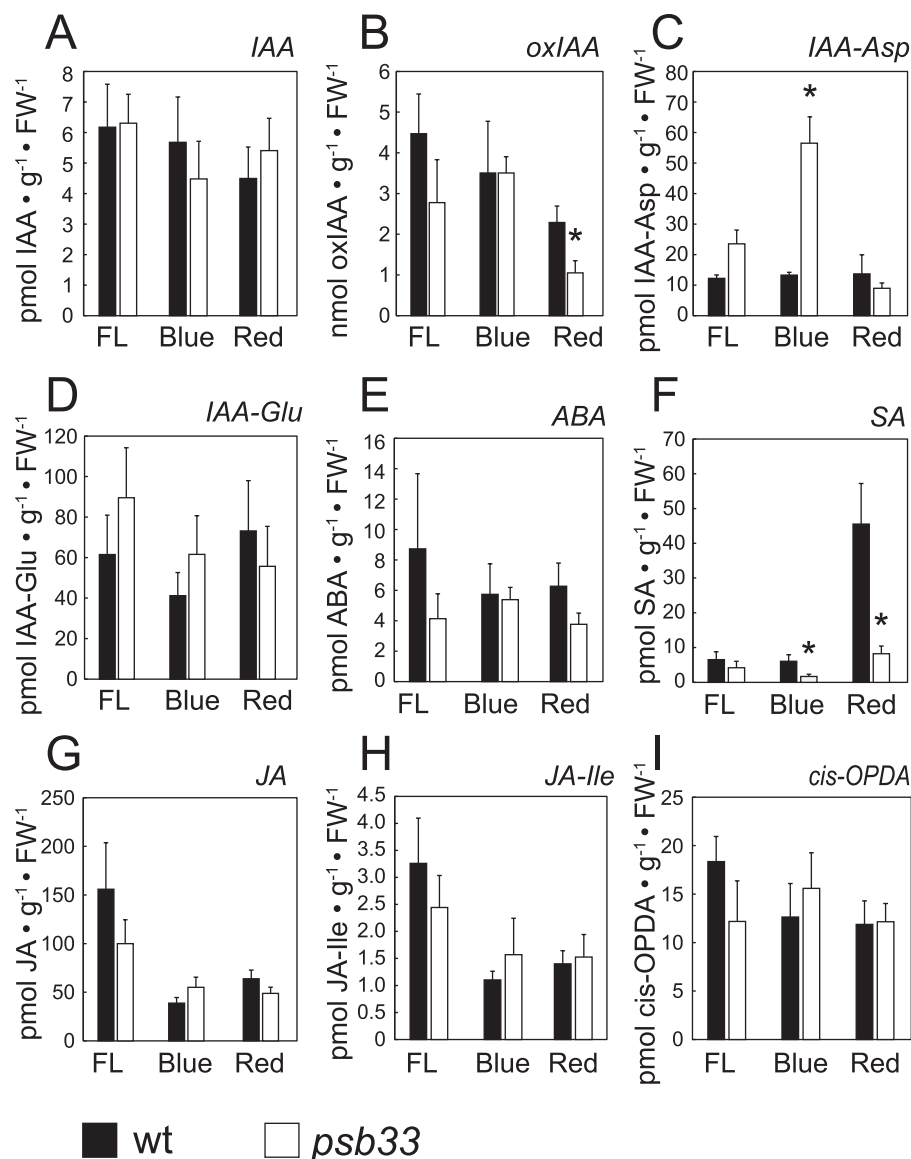
Fig. 3. Changes in phytohormone levels are observed in *psb33* grown in blue or red monochromatic light. Hormone levels were determined in leaf tissue (fresh weight, FW) from plants grown in fluorescent white light (FL) or under LED emitting light in different wavelengths of blue (400, 420, 440 nm) or red (630, 660 nm) light. Means and standard deviation are shown (*n*=4). Asterisks indicate a statistically significant difference in the mutant line (*psb33*) versus the wild type (WT) as determined by one-way ANOVA with Bonferroni–Holm *post hoc* test (*P*<0.01). (A) Indole acetic acid (IAA); (B) oxindole-3-IAA (oxIAA); (C) aspartic acid-conjugated IAA (IAA-Asp); (D) glutamate conjugated IAA (IAA-Glu); (E) abscisic acid (ABA); (F) salicylic acid (SA); (G) jasmonic acid (JA); (H) isoleucine conjugate JA (JA-Ile); (I) 12-oxo-phytodienoic acid (*cis*-OPDA).

in lights with UV-A (Fig. 5C; Supplementary Fig. S5). The F_v/F_m ratio of *psb33* plants grown in 420/450 nm light was significantly higher (one-way ANOVA, *P*<0.01) than in plants grown in 400 nm or 400/420/440 nm light (Fig. 5C). Thus, plants cultivated in light conditions lacking UV-A wavelengths performed better in terms of photosynthetic performance than plants grown in light containing UV-A.

Photosystem II core protein levels are reduced in psb33

The low F_v/F_m measured in the *psb33* mutant indicated decreased PSII efficiency and possibly damage to the PSII complex. We therefore examined potential photodamage to PSII in *psb33* grown in various blue light conditions. To investigate

if PSII and PSI protein levels were influenced by the quality of light, whole-leaf proteins were extracted from plants grown in either fluorescent white light or blue light with or without the 400 nm UV-A component (see Supplementary Fig. S4; 400/420/440 or 420/440 nm, respectively), and red light. Further, the fresh weight of plants was determined, and whole leaf proteins extracted from wild type and *psb33* plants grown under blue and red light in combination with far-red light (400/420/440/730 or 630/660/730 nm, respectively; Supplementary Fig. S6). Far-red light was included in the experimental set-up since it predominantly excites PSI. The far-red light treatment could thus reveal if increased excitation pressure of PSI would balance the relative energy distribution between the two photosystems and reduce photodamage. Extracted whole leaf proteins were separated on SDS-PAGE,
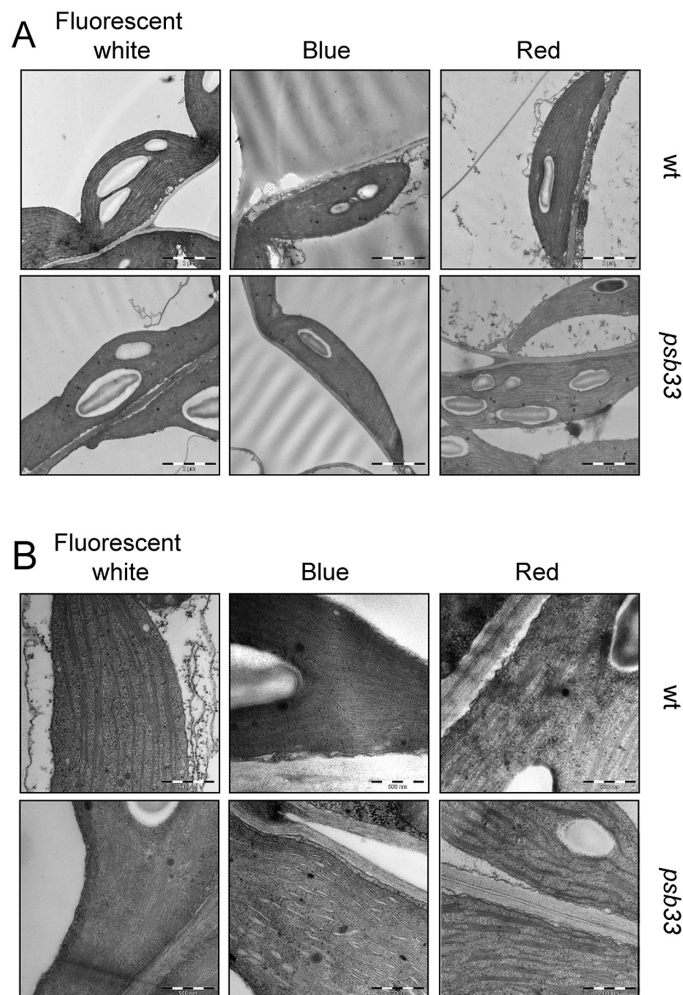
cannot alone explain the blue light growth phenotype. The PSII core proteins D1 and D2 were both reduced in *psb33* in blue light conditions. The corresponding reduction in protein abundance occurred in *psb33* exposed to 400 nm LED light, whereas plants exposed to 420/440 nm light displayed higher levels of D1 than plants from only 400 nm or 400/420/440 nm light (Fig. 6A, B).

Photosystem II electron transport properties are modified in psb33

The reduced levels of the D1 and D2 proteins in *psb33* cultivated under UV-A light may indicate an altered redox state of the acceptor side of PSII. To investigate this, we performed flash–induced variable fluorescence decay and thermoluminescence measurements in isolated PSII membranes from wild type and *psb33* plants. Analysis of the flash-induced fluorescence decay kinetics demonstrated faster electron transfer from Q_A^- to Q_B in *psb33* mutant (Fig. 7A, left panel) (Vass *et al.*, 1999; Mamedov *et al.*, 2000; Roose *et al.*, 2010). Also, thermoluminescence measurements, which are a useful complement to the flash-induced fluorescence decay measurements (Vass and Govindjee, 1996; Ducruet and Vass, 2009), also showed the presence of only a slightly up-shifted B-band (which represents the $Q_B^-{\to}S_2$ state recombination) at 38 °C. This is different compared with a mixture of the Q-band (which represents the $Q_A^-{\to}S_2$ state recombination) and B-band, present in thylakoids from wild type at 14 and 36 °C (Fig. 7B, left panel). Thus, both measurements confirm the presence of a more oxidized acceptor side of PSII and a higher redox potential of Q_B in *psb33* mutant.

The fluorescence decay kinetics and thermoluminescence bands measured in the presence of 3-(3,4-dichlorophenyl)–1,1-dimethylurea (DCMU) (and in the case of thermoluminescence indicating only the $Q_A^-{\to}S_2$ state recombination) were virtually the same in the wild type and *psb33* mutant (Fig. 7A and B, respectively, right panel). This indicated that the redox properties of Q_A and the water oxidizing complex on the donor side of PSII were not affected in the *psb33* mutant. This was also corroborated by EPR spectroscopy measurements of the S_2 state multiline signal, which were found to be similar in wild type and *psb33* mutant (Fig. 7D).

Interestingly, cytochrome b_{559}, an integral part and an alternative electron donor/acceptor of the PSII reaction center (Shinopoulos and Brudvig, 2012) was found to be predominantly in the low potential form in the *psb33* mutant (Fig. 7E) again, indicating a more oxidized acceptor side in PSII. However, the overall amount of the PSII reaction centers, as judged from the tyrosine D radical on a chlorophyll basis, was only slightly diminished in the *psb33* mutant (Fig. 7C).

psb33 *reactive oxygen species levels are unaffected by UV-A light*

The redox potential of Q_B is important for the regulation of electron transfer for both forward and backward electron transfer, which functions as a protective mechanism for PSII (Kato *et al.*, 2016). The modulated potential of Q_B
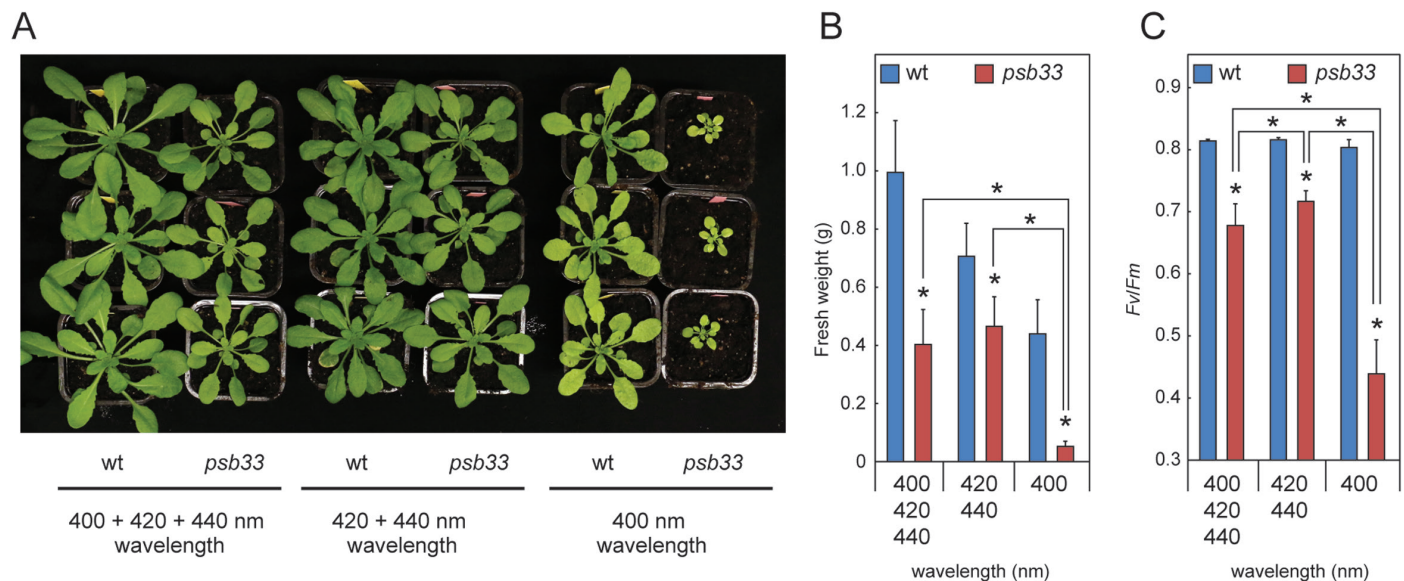

Fig. 4. Thylakoid ultrastructure of *psb33* and wild type plants grown in different light conditions. Representative transmission electron micrographs are shown for leaf chloroplasts from 5-week-old wild type (WT) and *psb33* mutant plants fixed 2 h after the onset of illumination. The thylakoids of the wild type and *psb33* mutant are similar when grown in fluorescent white light or under LED emitting red light at the wavelength of 630/660 nm. When grown under LED emitting blue light (400, 420, 450 nm), *psb33* displays swollen thylakoid, rarely observed in the wild type. Scale bars, 2 µm (A) and 500 nm (B).

immunoblotted, and labeled with antibodies specific for PSII (D1 and D2), PSI (PsaA and PsaB), LHCII (Lhcb1 and Lhcb2) and its phosphorylated forms (Lhcb1-P and Lhcb2-P) and Rubisco large subunit (RbcL) (Supplementary Fig. S7A). PsaA and PsaB levels varied in the different light conditions but were largely similar between wild type and *psb33*. So was the abundance of RbcL. In agreement with the impaired state transition phenotype of *psb33*, phosphorylation of Lhcb1 and Lhcb2 was almost completely lost in the *psb33* mutant in blue light. Notably, in red light and light supplemented with far-red, Lhcbs were phosphorylated to a certain level in *psb33* plants.

Furthermore, very little phosphorylation of Lhcb proteins was observed in *psb33* in fluorescent white light, corroborating our previous findings (Fristedt *et al.*, 2017). Our compiled data thus indicated that the redistribution of energy between the two photosystems through rearrangement of the LHCII light-harvesting antenna is impaired in *psb33*. Yet, this deficiency

A

wt   *psb33*   wt   *psb33*   wt   *psb33*

400 + 420 + 440 nm   420 + 440 nm   400 nm
wavelength   wavelength   wavelength

B

C

Fig. 5. *psb33* plants are sensitive to UV-A light. Plants were grown for 2 weeks in fluorescent white light and then transferred to LED emitting blue light in different wavelengths (400, 400/420, or 400/420/440 nm) but with similar intensity (120 PFD) where they were grown for 3 more weeks before photographs were taken (A), fresh weight determined (B), and F_v/F_m measured (C). Means and standard deviation are shown where $n=13–15$ (B) and $n=18–21$ (C). Asterisks indicate statistically significantly different from wild type under the specified growth condition or between samples marked by brackets (one-way ANOVA, Bonferroni–Holm *post hoc* test, $P<0.01$). Data used for statistical analysis of fresh weight were transformed (square root) to meet equal variance. (This figure is available in color at *JXB* online.)

in combination with elevated excitation pressure on PSII via UV-A light, could induce ROS-mediated damage to D1 and D2 in *psb33* mutant plants. To test this, we investigated if *psb33* mutant plants differed in ROS levels compared with wild type plants in UV-A light. Plants grown in 400 or 420/450 nm light were stained for hydrogen peroxide using 3,3′-diaminobenzidine and superoxide ($O_2 \cdot^-$) radicals using nitroblue tetrazolium (NBT). Surprisingly, no visual differences in levels of either H_2O_2 by DAB or $O_2 \cdot^-$ by NBT were observed between wild type and *psb33* (Fig. 8).

Discussion

The mechanisms by which plants maintain and optimize photosynthesis in fluctuating light environments are rapidly being unraveled (Tikkanen *et al.*, 2010, 2012; Cruz *et al.*, 2016; Vialet-Chabrand *et al.*, 2017). But as natural light fluctuates in intensity, it also varies considerably in quality, and the influence of light color in photosynthetic regulation has so far largely been overlooked (Allorent and Petroutsos, 2017). In this study, we demonstrate that plants lacking PSB33 are particularly sensitive to light in the UV-A spectral region. UV-A light was found to induce a dwarf phenotype in *psb33* plants, which was associated with diminished PSII protein levels.

PSB33 has a specific spectral influence on photosystem II and linear electron flow

Since the growth phenotype of the *psb33* mutant appeared to be very variable and strictly dependent on light conditions in our different growth facilities, we decided to place particular emphasis on the light quality in inducing the *psb33* phenotype

in this work. By cultivating the mutant in different light settings, it was found that the reduced growth of *psb33* was specifically induced by blue light (Fig. 1; Supplementary Fig. S3), particularly the spectral region that comprises the UV-A (Fig. 5). We therefore suggest that the previously reported growth phenotype, reaching approximately 50% the size of the wild type under normal growth conditions (Fristedt *et al.*, 2015), was due to the presence of short-wavelength blue light in the light source of the growth chambers.

The slow-growth of *psb33* in blue light was found to be connected to low levels of PSII core proteins D1 and D2 (Fig. 6), which inevitably leads to reduced photosynthesis rate. The effect was more pronounced in UV-A (400 nm) blue light than in 420/450 or 400/420/450 nm blue light at the same total photon flux (Fig. 6B). The red light did not cause any difference in D1 or D2 protein abundance between wild type and mutant. It is interesting to note that both blue and red light-grown plants displayed a similar reduction in maximal PSII quantum yield (F_v/F_m) (Fig. 2) and PI$_{ABS}$ (see Supplementary Fig. S3). However, *psb33* plants grown in exclusively blue light at 400 nm showed further reduced F_v/F_m values (Fig. 5C).

Supplementing UV-A containing blue light with far-red light rescued the phenotype to some extent in terms of both growth and PSII protein levels (Fig. 6A; Supplementary Fig. S6). As far-red light predominantly excites PSI, a possible explanation for this rescue is that PSB33 has a role in the linear electron transport chain to balance the redox components between the two photosystems. In the absence of PSB33, an unbalance of redox components in the electron transport chain would initiate the production of ROS, resulting in elevated PSII damage. However, we did not observe an increase of ROS in leaves from plants grown in UV-A light that would support an overexcitation of PSII and consequently increased
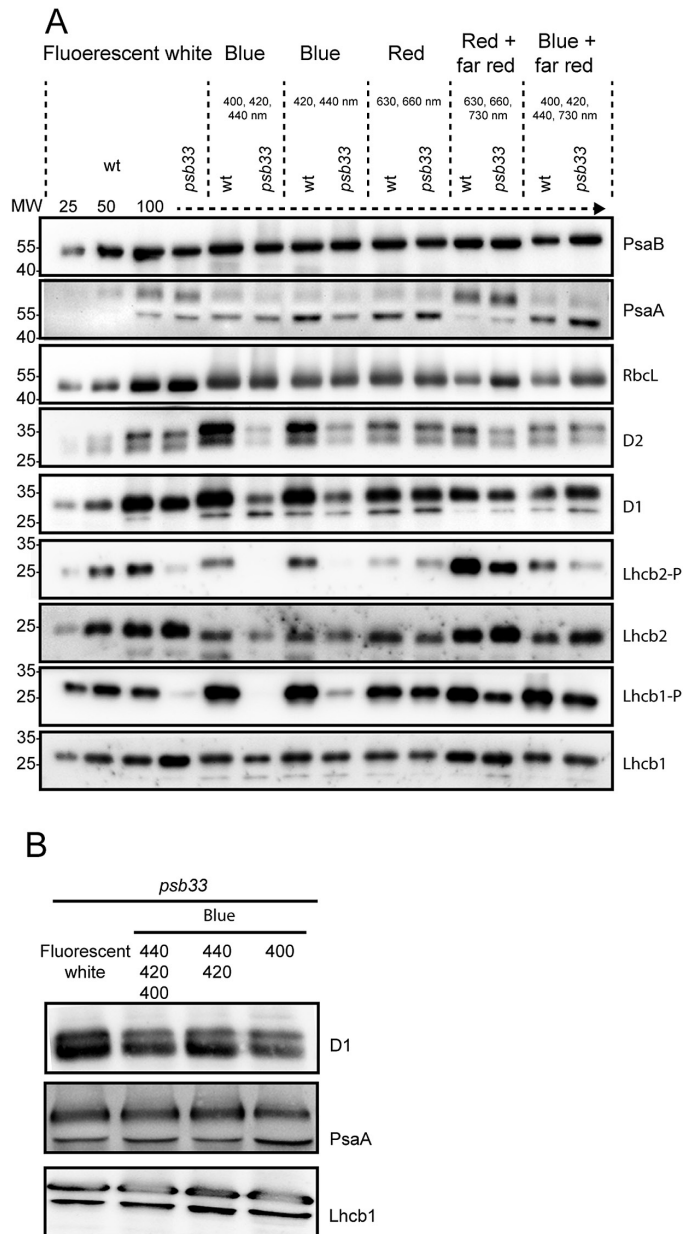
A

B

Fig. 6. Western blots of total protein extracts from plants grown in different light conditions. Whole leaf protein extracts were prepared from plants grown for 3 weeks in either fluorescent white light or under LED emitting light in different wavelengths of (A) blue light (400/420/440 or 420/440 nm), red light (630/650 nm), and blue and red light supplemented with far-red light (400/420/440/730 or 630/650/730 nm) and (B) blue light (400, 420/440 or 400/420/440 nm). Proteins were separated with SDS-PAGE, and loading was based on chlorophyll content.

photodamage. Another, perhaps more likely explanation is that the rescue effect of far-red is a consequence of reduced UV-A blue light as the total photon flux was kept constant in the experiments (i.e. 50% of the total light was provided by far-red and 50% by blue light).

When we tested mutants with reported impaired ability for PSII superstructure (*psbw*), state transitions (*lhcb1*, *lchb2*, *psal*, and *stn7/8*), cyclic electron transport and proton gradient (*pgr5*), or NPQ (*npq4*), none exhibited a slow-growth phenotype comparable to that of *psb33* in blue light, indicating that PSB33 has a unique role in blue light

perception unrelated to these known pathways to maintain photosynthesis.

Saliccylic acid and aspartic acid-conjugated indole-3-acetic acid hormone levels differ in psb33 plants exposed to different lights

SA levels are well known to influence plant growth negatively and to be important for light acclimation (Rivas-San Vicente and Plasencia, 2011). Surprisingly, the SA level decreased in response to both blue and red light treatments in *psb33*, whereas it increased in the wild type (Fig. 3F). SA and glutathione interplay to regulate antioxidant response through ROS scavenging (Herrera-Vásquez *et al.*, 2015). The low levels of SA in *psb33* could accordingly explain the accumulation of different ROS in the mutant line, as previously reported (Fristedt *et al.*, 2015). However, we could not observe any differences between wild type and *psb33* in or the absence of UV-A light (400 and 420/450 nm, respectively) in terms of H_2O_2 and superoxide radicals (Fig. 8), suggesting that changed SA and ROS levels did not contribute to the deleterious effect of UV-A light. The only hormonal change exclusively observed in *psb33* grown in blue light was a strong accumulation of aspartic acid–conjugated IAA (IAA-Asp) (Fig. 3C). This is believed to be an inactive form of IAA that is destined for catabolism (Woodward and Bartel, 2005; Ludwig-Müller, 2011).

psb33 plants grown in blue light show an abnormal thylakoid ultrastructure

PSB33 is primarily located in non-appressed thylakoid regions (Fristedt *et al.*, 2015; Fristedt *et al.*, 2017; Kato *et al.*, 2017). Quality control of PSII is dependent on reversible thylakoid structure dynamics (Yamamoto, 2016). Light induces a reversible swelling and unstacking of the thylakoids, which is necessary for proper PSII repair and protects PSII from damage (Khatoon *et al.*, 2009). Furthermore, the increased surface area of the membranes influences its fluidity, which is important for lateral movement of proteins and other compounds within the membrane regulating NPQ, state transition, and PSII repair (Yamamoto, 2016). Integrated regulation of the many processes involved in the dynamics of the thylakoid membrane is not yet fully understood (Tikkanen and Aro, 2014). It has been shown that the PSII–LHCII supercomplex phosphorylation level affects the distance between the grana stacks as well as their size, and it been suggested that complexes in opposite orientation repel each other, causing unstacking of the grana (Fristedt *et al.*, 2009). Thus, the reduced levels of PSII (D1 and D2) observed in *psb33* mutant plants exposed to blue light (Fig. 6) could explain changes to the thylakoid structure of *psb33*, seen by transmission electron microscopy (Fig. 4). The distinctly swollen stroma lamella might negatively influence the rate of movement of proteins and compounds, restrict PSII quality control, and enhance damage to the complex (Kirchhoff, 2014). The altered PSII superstructure and PSII level in *psb33* might have further enhanced the growth phenotype.
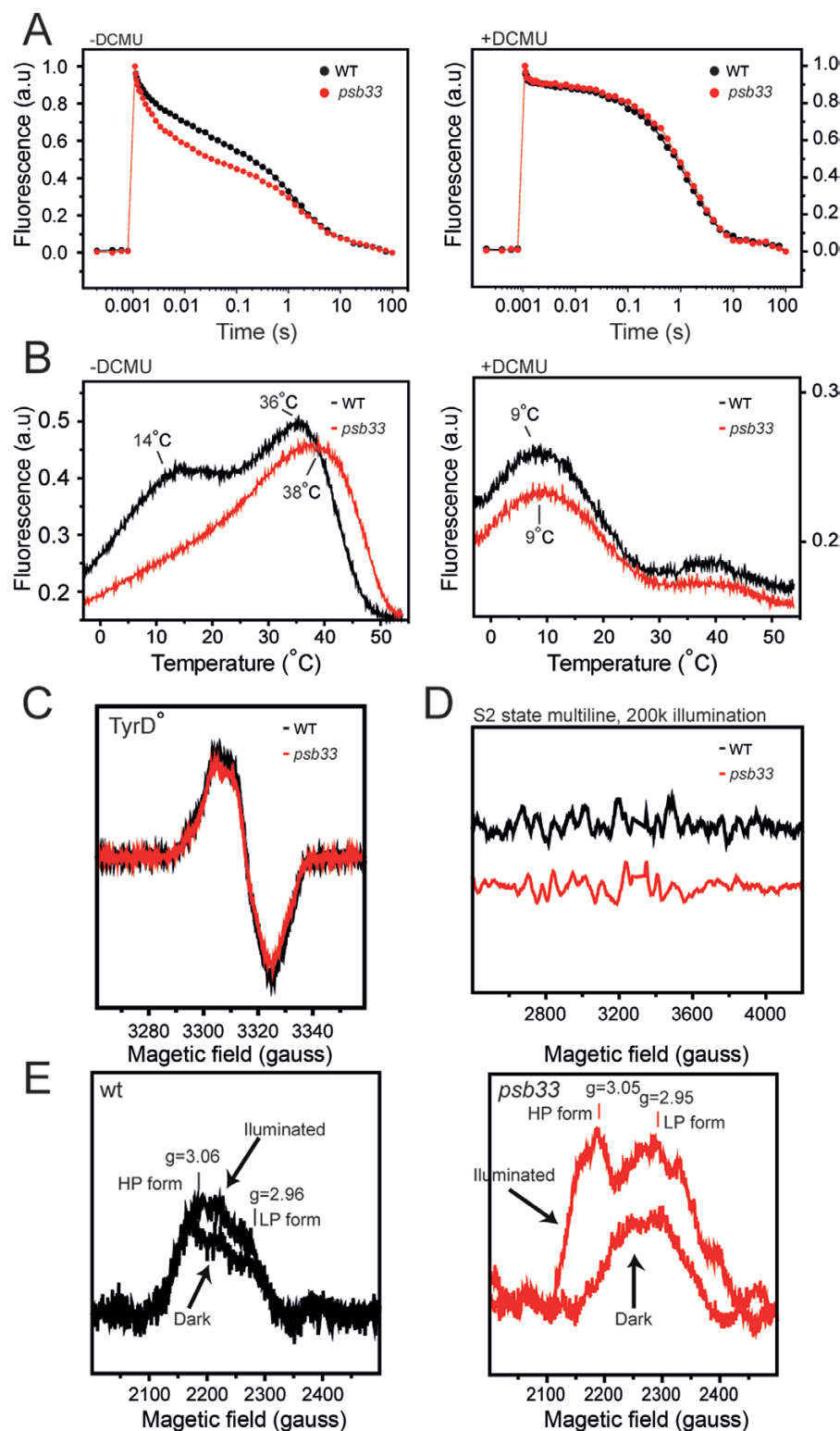
Fig. 7. Analysis of electron transport components in photosystem II from thylakoid membranes from WT and *psb33* mutant. (A) Flash-induced fluorescence decay kinetic in the absence (left panel) or the presence (right panel) of 20 µM DCMU. (B) Thermoluminescence glow curves in the absence (left panel) or the presence (right panel) of 40 µM DCMU. (C–E) EPR spectroscopy measurements of the tyrosine D radical (C), the S_2 state of the water oxidizing complex (D), and the oxidized form of cytochrome b_{559} in the g_z region (E) before and after illumination at 77 K. The low and high potential of cytochrome b_{559} are marked as HP and LP, respectively. EPR conditions: microwave frequency: 9.35 GHz, microwave power 1.3 µW, and temperature 15 K for (C), 10 mW and 7 K for (D), and 5 mW and 15 K for (E). (This figure is available in color at *JXB* online.)

UV-A light reduces photosystem II proteins in psb33

Two previous observations have been linked to blue and UV-A light that can explain *psb33* dwarf phenotype. First, the Mn_4CaO_5 can directly absorb UV light and initiate the photoinactivation process (Ohnishi *et al.*, 2005). It is possible, but not likely, that PSB33 protects the Mn cluster, due to restricted access by the
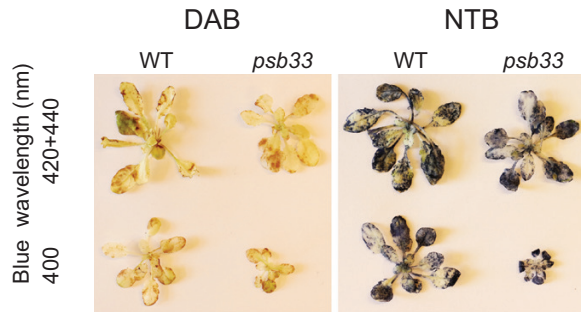
Fig. 8. ROS staining of plants grown in different wavelengths of blue light. Seven-day-old seedlings were transferred from fluorescent white light to LED plant growth chambers emitting light in different wavelengths of blue light (400 or 420/450 nm) and grown for 2 weeks before staining against H_2O_2 (3,3′-diaminobenzidine, DAB) and superoxide radicals (nitroblue tetrazolium, NTB). The photographs show representatives from five to eight stained plants. (This figure is available in color at *JXB* online.)

OEC proteins. However, our data on intra-PSII electron flow do not support this hypothesis (Fig. 7). Second, blue and UV-A light-mediated signals have been linked to increased D2 and CP43 gene expression in mature chloroplasts (Christopher and Mullet, 1994) and this is consistent with our results: we observed an up-regulation of D1 and D2 PSII proteins in wild type plants exposed to blue/UV-A light (Fig. 6A). In contrast, D1 and D2 were down-regulated in *psb33* mutant plants in blue/UV-A.

PSB33's location is largely in non-appressed thylakoid regions, with its head domain exposed to the stroma (Fristedt *et al.*, 2015), and it is part of a larger protein complex (Fristedt *et al.*, 2017). PSB33 is likely part of a signaling mechanism involved in the rejuvenation of PSII. A hypothetical scenario would be that this mechanism is either triggered by UV-A light or develops as a consequence of plant exposure to blue and UV light, possibly as a result of re-adjusted redox regulation. Such a signaling cascade may eventually induce a conformational change on PSB33, which triggers downstream signaling for transcription of various PSII proteins.

Conclusions

The accumulated data show that PSB33 has an important role in sustaining a functional PSII pool in blue light, especially in UV-A light. Although the severe growth phenotype of *psb33* plants in blue light is connected to misregulated phosphorylation and migration of Lhcb proteins, this appears not to be a causal relationship. The exact molecular mechanism of how PSB33 protein senses UV-light and initiates the photosynthetic response remains to be investigated.

Supplementary data

Supplementary data are available at *JXB* online.

Fig. S1. Wild type and *psb33* plants grown in white fluorescent light for 4 weeks at 140 μmols m^{-2} s^{-1}.

Fig. S2. Wild type, *psb33*, and *stn7stn8* plants grown for 15 d under white fluorescent light at 120 μmols m^{-2} s^{-1}.

Fig. S3. PI$_{ABS}$ in wild type, *psb33*, and *stn7stn8* plants grown in blue and red light.

Fig. S4. Full-spectrum of 400 nm LED light source.

Fig. S5. Wild type and *psb33* plants grown in 385 nm UV-A light.

Fig. S6. Wild type and *psb33* plants grown in blue or red light combined with far-red.

Fig. S7. PI$_{ABS}$ in wild type and *psb33* plants grown in three different blue light conditions.

Acknowledgements

Author contributions

AN and BLB designed the experiments. AN, DB, and BLB performed light experiments and growth of plants. AN and BLB performed pigment, chlorophyll *a* fluorescence, thylakoid membrane preparation, SDS-PAGE, immunoblotting, and ROS determination. AP and ON performed hormonal analysis. OJ performed transmission electron microscopy. FM performed thermoluminescence and low-temperature electron paramagnetic resonance spectroscopy. All authors contributed to the analysis of results and writing of the manuscript.

Conflict of interest

BLB is employed at AstraZeneca, Respiratory & Immunology at the time of publication and declares that there is no conflict of interest that has effected this publication.

Data availability

The data supporting the findings of this study are available from the corresponding author, BLB, upon request.

References

Adamska I, Kloppstech K, Ohad I. 1992. UV light stress induces the synthesis of the early light-inducible protein and prevents its degradation. The Journal of Biological Chemistry **267**, 24732–24737.

Allen JF, Bennett J, Steinback KE, Arntzen CJ. 1981. Chloroplast protein phosphorylation couples plastoquinone redox state to distribution of excitation energy between photosystems. Nature **291**, 25–29.

Allorent G, Lefebvre-Legendre L, Chappuis R, Kuntz M, Truong TB, Niyogi KK, Ulm R, Goldschmidt-Clermont M. 2016. UV-B photoreceptor-mediated protection of the photosynthetic machinery in *Chlamydomonas reinhardtii*. Proceedings of the National Academy of Sciences, USA **113**, 14864–14869.

Allorent G, Petroutsos D. 2017. Photoreceptor-dependent regulation of photoprotection. Current Opinion in Plant Biology **37**, 102–108.

Aro EM, Virgin I, Andersson B. 1993. Photoinhibition of Photosystem II. Inactivation, protein damage and turnover. Biochimica et Biophysica Acta **1143**, 113–134.

Bellafiore S, Barneche F, Peltier G, Rochaix JD. 2005. State transitions and light adaptation require chloroplast thylakoid protein kinase STN7. Nature **433**, 892–895.

Bonardi V, Pesaresi P, Becker T, Schleiff E, Wagner R, Pfannschmidt T, Jahns P, Leister D. 2005. Photosystem II core phosphorylation and photosynthetic acclimation require two different protein kinases. Nature **437**, 1179–1182.

Cazzaniga S, Dall' Osto L, Kong SG, Wada M, Bassi R. 2013. Interaction between avoidance of photon absorption, excess energy dissipation and zeaxanthin synthesis against photooxidative stress in Arabidopsis. The Plant Journal **76**, 568–579.

Chaiwanon J, Wang W, Zhu JY, Oh E, Wang ZY. 2016. Information integration and communication in plant growth regulation. Cell **164**, 1257–1268.

Chen G, Allahverdiyeva Y, Aro EM, Styring S, Mamedov F. 2011. Electron paramagnetic resonance study of the electron transfer reactions in photosystem II membrane preparations from *Arabidopsis thaliana*. Biochimica et Biophysica Acta **1807**, 205–215.

Christie JM, Blackwood L, Petersen J, Sullivan S. 2015. Plant flavoprotein photoreceptors. Plant & Cell Physiology **56**, 401–413.

Christopher DA, Mullet JE. 1994. Separate photosensory pathways co-regulate blue light/ultraviolet-A-activated psbD-psbC transcription and light-induced D2 and CP43 degradation in barley (*Hordeum vulgare*) chloroplasts. Plant Physiology **104**, 1119–1129.

Cruz JA, Savage LJ, Zegarac R, Hall CC, Satoh-Cruz M, Davis GA, Kovac WK, Chen J, Kramer DM. 2016. Dynamic environmental photosynthetic imaging reveals emergent phenotypes. Cell Systems **2**, 365–377.

Daudi A, O'Brien JA. 2012. Detection of hydrogen peroxide by DAB staining in *Arabidopsis* leaves. Bio-protocol **2**, e263.

Ducruet JM, Vass I. 2009. Thermoluminescence: experimental. Photosynthesis Research **101**, 195–204.

Floková K, Tarkowská D, Miersch O, Strnad M, Wasternack C, Novák O. 2014. UHPLC-MS/MS based target profiling of stress-induced phytohormones. Phytochemistry **105**, 147–157.

Folta KM, Kaufman LS. 1999. Regions of the pea *Lhcb1**4 promoter necessary for blue-light regulation in transgenic Arabidopsis. Plant Physiology **120**, 747–756.

Fristedt R, Herdean A, Blaby-Haas CE, Mamedov F, Merchant SS, Last RL, Lundin B. 2015. PHOTOSYSTEM II PROTEIN33, a protein conserved in the plastid lineage, is associated with the chloroplast thylakoid membrane and provides stability to photosystem II supercomplexes in Arabidopsis. Plant Physiology **167**, 481–492.

Fristedt R, Trotta A, Suorsa M, Nilsson AK, Croce R, Aro EM, Lundin B. 2017. PSB33 sustains photosystem II D1 protein under fluctuating light conditions. Journal of Experimental Botany **68**, 4281–4293.

Fristedt R, Vener AV. 2011. High light induced disassembly of photosystem II supercomplexes in Arabidopsis requires STN7-dependent phosphorylation of CP29. PLoS One **6**, e24565.

Fristedt R, Willig A, Granath P, Crèvecoeur M, Rochaix JD, Vener AV. 2009. Phosphorylation of photosystem II controls functional macroscopic folding of photosynthetic membranes in *Arabidopsis*. The Plant Cell **21**, 3950–3964.

García-Cerdán JG, Kovács L, Tóth T, Kereïche S, Aseeva E, Boekema EJ, Mamedov F, Funk C, Schröder WP. 2011. The PsbW protein stabilizes the supramolecular organization of photosystem II in higher plants. The Plant Journal **65**, 368–381.

Goh CH. 2009. Phototropins and chloroplast activity in plant blue light signaling. Plant Signaling & Behavior **4**, 693–695.

Hakala M, Tuominen I, Keränen M, Tyystjärvi T, Tyystjärvi E. 2005. Evidence for the role of the oxygen-evolving manganese complex in photoinhibition of photosystem II. Biochimica et Biophysica Acta **1706**, 68–80.

Herdean A, Teardo E, Nilsson AK, et al. 2016. A voltage-dependent chloride channel fine-tunes photosynthesis in plants. Nature Communications **7**, 11654.

Herrera-Vásquez A, Salinas P, Holuigue L. 2015. Salicylic acid and reactive oxygen species interplay in the transcriptional control of defense genes expression. Frontiers in Plant Science **6**, 171.

Jajoo A, Mekala NR, Tongra T, Tiwari A, Grieco M, Tikkanen M, Aro EM. 2014. Low pH-induced regulation of excitation energy between the two photosystems. FEBS Letters **588**, 970–974.

Johnson MP, Ruban AV. 2010. Arabidopsis plants lacking PsbS protein possess photoprotective energy dissipation. The Plant Journal **61**, 283–289.

Jones LW, Kok B. 1966. Photoinhibition of chloroplast reactions. I. Kinetics and action spectra. Plant Physiology **41**, 1037–1043.

Kalaji HM, Schansker G, Ladle RJ, et al. 2014. Frequently asked questions about *in vivo* chlorophyll fluorescence: practical issues. Photosynthesis Research **122**, 121–158.

Kanazawa A, Ostendorf E, Kohzuma K, et al. 2017. Chloroplast ATP synthase modulation of the thylakoid proton motive force: implications for photosystem I and photosystem II photoprotection. Frontiers in Plant Science **8**, 719.

Kato Y, Nagao R, Noguchi T. 2016. Redox potential of the terminal quinone electron acceptor QB in photosystem II reveals the mechanism of electron transfer regulation. Proceedings of the National Academy of Sciences, USA **113**, 620–625.

Kato Y, Sakamoto W. 2014. Phosphorylation of photosystem II core proteins prevents undesirable cleavage of D1 and contributes to the fine-tuned repair of photosystem II. The Plant Journal **79**, 312–321.

Kato Y, Yokono M, Akimoto S, Takabayashi A, Tanaka A, Tanaka R. 2017. Deficiency of the stroma-lamellar protein LIL8/PSB33 affects energy transfer around PSI in Arabidopsis. Plant & Cell Physiology **58**, 2026–2039.

Khatoon M, Inagawa K, Pospísil P, et al. 2009. Quality control of photosystem II: Thylakoid unstacking is necessary to avoid further damage to the D1 protein and to facilitate D1 degradation under light stress in spinach thylakoids. The Journal of Biological Chemistry **284**, 25343–25352.

Kirchhoff H. 2014. Diffusion of molecules and macromolecules in thylakoid membranes. Biochimica et Biophysica Acta **1837**, 495–502.

Kirilovsky D, Kerfeld CA. 2013. The Orange Carotenoid Protein: a blue-green light photoactive protein. Photochemical & Photobiological Sciences **12**, 1135–1143.

Kok B. 1956. On the inhibition of photosynthesis by intense light. Biochimica et Biophysica Acta **21**, 234–244.

Külheim C, Agren J, Jansson S. 2002. Rapid regulation of light harvesting and plant fitness in the field. Science **297**, 91–93.

Li L, Aro EM, Millar AH. 2018. Mechanisms of photodamage and protein turnover in photoinhibition. Trends in Plant Science **23**, 667–676.

Li XP, Muller-Moule P, Gilmore AM, Niyogi KK. 2002. PsbS-dependent enhancement of feedback de-excitation protects photosystem II from photoinhibition. Proceedings of the National Academy of Sciences, USA **99**, 15222–15227.

Lichtenthaler HK, Wellburn AR. 1983. Determinations of total carotenoids and chlorophylls a and b of leaf extracts in different solvents. Biochemical Society Transactions **11**, 591–592.

Long S, Humphries S, Falkowski PG. 1994. Photoinhibition of photosynthesis in nature. Annual Review of Plant Physiology and Plant Molecular Biology **45**, 633–662.

Ludwig-Müller J. 2011. Auxin conjugates: their role for plant development and in the evolution of land plants. Journal of Experimental Botany **62**, 1757–1773.

Lunde C, Jensen PE, Haldrup A, Knoetzel J, Scheller HV. 2000. The PSI-H subunit of photosystem I is essential for state transitions in plant photosynthesis. Nature **408**, 613–615.

Mamedov F, Stefansson H, Albertsson PA, Styring S. 2000. Photosystem II in different parts of the thylakoid membrane: a functional comparison between different domains. Biochemistry **39**, 10478–10486.

Mekala NR, Suorsa M, Rantala M, Aro EM, Tikkanen M. 2015. Plants actively avoid state transitions upon changes in light intensity: role of light-harvesting complex II protein dephosphorylation in high light. Plant Physiology **168**, 721–734.

Munekage Y, Hojo M, Meurer J, Endo T, Tasaka M, Shikanai T. 2002. PGR5 is involved in cyclic electron flow around photosystem I and is essential for photoprotection in *Arabidopsis*. Cell **110**, 361–371.

Ohad I, Kyle DJ, Arntzen CJ. 1984. Membrane protein damage and repair: removal and replacement of inactivated 32-kilodalton polypeptides in chloroplast membranes. The Journal of Cell Biology **99**, 481–485.

Ohnishi N, Allakhverdiev SI, Takahashi S, Higashi S, Watanabe M, Nishiyama Y, Murata N. 2005. Two-step mechanism of photodamage to photosystem II: step 1 occurs at the oxygen-evolving complex and step 2 occurs at the photochemical reaction center. Biochemistry **44**, 8494–8499.

Petroutsos D, Tokutsu R, Maruyama S, et al. 2016. A blue-light photoreceptor mediates the feedback regulation of photosynthesis. Nature **537**, 563–566.

Pietrzykowska M, Suorsa M, Semchonok DA, Tikkanen M, Boekema EJ, Aro EM, Jansson S. 2014. The light-harvesting chlorophyll

a/b binding proteins Lhcb1 and Lhcb2 play complementary roles during state transitions in *Arabidopsis*. The Plant Cell **26**, 3646–3660.

Porra R, Thompson W, Kriedemann P. 1989. Determination of accurate extinction coefficients and simultaneous equations for assaying chlorophylls *a* and *b* extracted with four different solvents: verification of the concentration of chlorophyll standards by atomic absorption spectroscopy. Biochimica et Biophysica Acta **975**, 384–394.

Pribil M, Pesaresi P, Hertle A, Barbato R, Leister D. 2010. Role of plastid protein phosphatase TAP38 in LHCII dephosphorylation and thylakoid electron flow. PLoS Biology **8**, e1000288.

Rintamäki E, Martinsuo P, Pursiheimo S, Aro EM. 2000. Cooperative regulation of light-harvesting complex II phosphorylation via the plastoquinol and ferredoxin-thioredoxin system in chloroplasts. Proceedings of the National Academy of Sciences, USA **97**, 11644–11649.

Rivas-San Vicente M, Plasencia J. 2011. Salicylic acid beyond defence: its role in plant growth and development. Journal of Experimental Botany **62**, 3321–3338.

Roose JL, Yocum CF, Popelkova H. 2010. Function of PsbO, the photosystem II manganese-stabilizing protein: probing the role of aspartic acid 157. Biochemistry **49**, 6042–6051.

Sarvikas P, Hakala M, Pätsikkä E, Tyystjärvi T, Tyystjärvi E. 2006. Action spectrum of photoinhibition in leaves of wild type and *npq1-2* and *npq4-1* mutants of *Arabidopsis thaliana*. Plant & Cell Physiology **47**, 391–400.

Schellenberger Costa B, Jungandreas A, Jakob T, Weisheit W, Mittag M, Wilhelm C. 2013. Blue light is essential for high light acclimation and photoprotection in the diatom *Phaeodactylum tricornutum*. Journal of Experimental Botany **64**, 483–493.

Scheller HV, Haldrup A. 2005. Photoinhibition of photosystem I. Planta **221**, 5–8.

Shapiguzov A, Ingelsson B, Samol I, Andres C, Kessler F, Rochaix JD, Vener AV, Goldschmidt-Clermont M. 2010. The PPH1 phosphatase is specifically involved in LHCII dephosphorylation and state transitions in *Arabidopsis*. Proceedings of the National Academy of Sciences, USA **107**, 4782–4787.

Shinopoulos KE, Brudvig GW. 2012. Cytochrome *b*559 and cyclic electron transfer within photosystem II. Biochimica et Biophysica Acta **1817**, 66–75.

Strasser RJ, Srivastava A, Tsimilli M. 2000. The fluorescence transient as a tool to characterize and screen photosynthetic samples. In: Yunus M, Pathre U, Mohanty P, eds. Probing Photosynthesis: Mechanism, Regulation & Adaptation. Boca Raton, London, New York: CRC Press, 445–483.

Strasser RJ, Tsimilli-Michael M, Srivastava A. 2004. Analysis of the chlorophyll a fluorescence transient. In: Papageorgiou GC, Govindjee, eds. Chlorophyll a fluorescence: A signature of photosynthesis. Dordrecht: Springer Netherlands, 321–362.

Suorsa M, Jarvi S, Grieco M, *et al.* 2012. PROTON GRADIENT REGULATION5 is essential for proper acclimation of *Arabidopsis*

photosystem I to naturally and artificially fluctuating light conditions. The Plant Cell **24**, 2934–2948.

Takahashi S, Milward SE, Yamori W, Evans JR, Hillier W, Badger MR. 2010. The solar action spectrum of photosystem II damage. Plant Physiology **153**, 988–993.

Tikkanen M, Aro EM. 2014. Integrative regulatory network of plant thylakoid energy transduction. Trends in Plant Science **19**, 10–17.

Tikkanen M, Grieco M, Kangasjärvi S, Aro EM. 2010. Thylakoid protein phosphorylation in higher plant chloroplasts optimizes electron transfer under fluctuating light. Plant Physiology **152**, 723–735.

Tikkanen M, Grieco M, Nurmi M, Rantala M, Suorsa M, Aro EM. 2012. Regulation of the photosynthetic apparatus under fluctuating growth light. Philosophical Transactions of the Royal Society of London. Series B, Biological Sciences **367**, 3486–3493.

Tikkanen M, Nurmi M, Kangasjärvi S, Aro EM. 2008. Core protein phosphorylation facilitates the repair of photodamaged photosystem II at high light. Biochimica et Biophysica Acta **1777**, 1432–1437.

Trotta A, Suorsa M, Rantala M, Lundin B, Aro EM. 2016. Serine and threonine residues of plant STN7 kinase are differentially phosphorylated upon changing light conditions and specifically influence the activity and stability of the kinase. The Plant Journal **87**, 484–494.

Vass I, Govindjee. 1996. Thermoluminescence from the photosynthetic apparatus. Photosynthesis Research **48**, 117–126.

Vass I, Kirilovsky D, Etienne AL. 1999. UV-B radiation-induced donor- and acceptor-side modifications of photosystem II in the cyanobacterium *Synechocystis* sp. PCC 6803. Biochemistry **38**, 12786–12794.

Vialet-Chabrand S, Matthews JS, Simkin AJ, Raines CA, Lawson T. 2017. Importance of fluctuations in light on plant photosynthetic acclimation. Plant Physiology **173**, 2163–2179.

Volgusheva A, Kruse O, Styring S, Mamedov F. 2016. Changes in the photosystem II complex associated with hydrogen formation in sulfur deprived *Chlamydomonas reinhardtii*. Algal Research **18**, 296–304.

Wang H, Wang H. 2015. Phytochrome signaling: time to tighten up the loose ends. Molecular Plant **8**, 540–551.

Woodward AW, Bartel B. 2005. Auxin: regulation, action, and interaction. Annals of Botany **95**, 707–735.

Yamamoto Y. 2016. Quality control of photosystem II: The mechanisms for avoidance and tolerance of light and heat stresses are closely linked to membrane fluidity of the thylakoids. Frontiers in Plant Science **7**, 1136.

Yoshioka-Nishimura M, Yamamoto Y. 2014. Quality control of photosystem II: the molecular basis for the action of FtsH protease and the dynamics of the thylakoid membranes. Journal of Photochemistry and Photobiology. B, Biology **137**, 100–106.

Zavafer A, Chow WS, Cheah MH. 2015. The action spectrum of photosystem II photoinactivation in visible light. Journal of Photochemistry and Photobiology. B, Biology **152**, 247–260.